Desalination and Water Treatment
www.deswater.com

doi: 10.1080/19443994.2016.1156031

57 (2016) 25757–25764
November

Taylor & Francis
Taylor & Francis Group

Complex doping of d-block elements cobalt, nickel and cadmium in magneso-silicate composite and its use in the treatment of aqueous waste

M.M. Abou-Mesalam[a,*], M.R. Abass[a], M.A. Abdel-Wahab[a], E.S. Zakaria[a], A.M. Hassan[b], H.F. Khalil[b]

[a] *Atomic Energy Authority, Hot Labs, Centre, P. Code 13759, Cairo, Egypt, emails: mabumesalam@yahoo.com (M.M. Abou-Mesalam), mohamed.ragab2014300@yahoo.com (M.R. Abass), mabumesalam@hotmail.com (M.A. Abdel-Wahab), essam_zakaria@yahoo.com (E.S. Zakaria)*
[b] *Faculty of Science, Al-AZhar University, Cairo, Egypt, emails: alimhassanuk@yahoo.co.uk (A.M. Hassan), Hazem.khalil@azhar.edu.eg (H.F. Khalil)*

Received 18 January 2016; Accepted 14 February 2016

ABSTRACT

Magneso-silicate and metal *in situ* doping composites have been synthesized by sol–gel technique. The structure of these composites was established by chemical analysis, X-ray diffraction, thermogravimetric, and differential thermal analyses, Fourier transform infrared spectroscopy and X-ray fluorescence analysis. Magneso-silicate and *in situ* doping of nickel, cobalt, and cadmium composites were found to have the formulas $MgSi_{4.26}O_{9.53}\cdot 2.17\ H_2O$, $Ni_{2.36}Mg_{0.043}Si_{2.91}O\cdot 1.29\ H_2O$, $Co_{1.45}Mg_{0.03}Si_{2.7}O\cdot 1.26\ H_2O$, and $CdMg_{0.059}Si_{1.24}O_{1.12}\cdot 0.83\ H_2O$, respectively. The capacities of these materials for some heavy metals such as Ni^{2+}, Co^{2+}, and Cd^{2+} were investigated and the data obtained showed that magneso-silicate has a higher capacity for the cations compared to *in situ* doping of heavy metal composites. Distribution coefficients in nitric acid medium have been evaluated to explore the separation potentiality of magneso-silicate for Ni^{2+}, Co^{2+}, and Cd^{2+} ions. Sorption isotherms for all cations were investigated and the data showed the applicability of Freundlich isotherm for all cases.

Keywords: Magneso-silicate; *In-situ*; Distribution; Capacity; Isotherm

1. Introduction

Nowadays, inorganic ion-exchange materials play an important role in analytical chemistry, based originally on their thermal and radiation resistance as well as their chemical attack [1]. The development of new inorganic ion exchangers with characteristic properties still needs attention and their utility in diverse fields is yet to be explored. Synthetic ion exchangers are used for a wide range of different application, ranging from environmental remediation [2,3], water softening [3], hydrometallurgy [3], biochemistry [4], catalysis [5], and selective adsorption [6,7] to medical applications [8]. Abou-Mesalam and El-Naggar have synthesized different inorganic ion-exchange materials based on silicate salts prepared [6,9] and used for removal of some heavy metals from industrial and hazardous wastes.

In this work, magneso-silicate and its doping with some heavy metals such as nickel, cobalt, and cadmium as inorganic ion-exchange materials were synthesized using sol–gel technique. The doping

---

*Corresponding author.

materials were investigated using different analytical technique and represented a new ion-exchange character compared the original ones. Structure formulas and analytical applications of magneso-silicate and its dopants for the recovery of some heavy metal from the aqueous waste solution were conducted.

2. Experimental

All reagents and chemicals used were of analytical grade and used without further purifications.

2.1. Synthesis of magneso-silicate composite

Magneso-silicate ion-exchange material was synthesized as reported earlier by Abou-Mesalam and El-Naggar. [6,9] by the dropwise addition of equimolar solutions (0.05 M) of magnesium chloride to sodium metasilicate with volumetric ratio for (Mg/Si) equal 1.5 with continuous stirring in a water bath adjusted at 60 ± 1˚C. The mixed solutions were immediately hydrolyzed in demineralized water. Diluted ammonia solution was added to the mixture until complete precipitation attained. The precipitate formed was kept in the mother solution to overnight standing. The precipitate was washed several times with distilled water, and then washed by 0.1 M HNO_3 to remove impurities and Cl^- ions. The precipitate is rewashed by distilled water to remove NO_3^- ions. After drying at 60 ± 1˚C, solid was poured in near boiling distilled water heated at 80 ± 1˚C to break the solid and remove air trapped inside the solid, then redried at 60 ± 1˚C. The obtained solid was grained and stored at room temperature.

2.2. In-situ doping magneso-silicate composite

Doping of some heavy metal such as Ni^{2+}, Co^{2+}, and Cd^{2+} ions with magneso-silicate ion-exchange material was synthesized as reported earlier [6,9] by the dropwise addition of equimolar solutions (0.05 M) of magnesium chloride to sodium metasilicate and MCl_2 with volumetric ratio 1:1.5:1 for M: Mg: Si, where M is Ni^{2+}, Co^{2+}, and Cd^{2+} ions with continuous stirring in a water bath adjusted at 60 ± 1˚C. The mixed solutions were immediately hydrolyzed in demineralized water with the same procedure as magneso-silicate prepared.

2.3. Composition and characterization of synthesized composites

The stiochiometry of the constituents in magneso-silicate and metal *in situ* doping composites were determined using Philips sequent ion X-ray spectrometer-2400. The solid samples were ground to very fine powders and then mixed with polyvinyl methacrylate as a binder to facilitate the pressing process. The mixture was pressed in a sample holder of 40 mm diameter aluminum cups and pressed on pressing machine at 20 psi to produce a sample with the diameter of 40 and 50 mm thickness. The concentrations of magnesium, silicone, nickel, cobalt, and cadmium were measured according to Super-Q quantitative application program.

Samples of magneso-silicate and metal *in situ* doping composites (20 mg) were analyzed for DTA and TGA with sample holder made of Al_2O_3 in N_2 atmosphere using a Shimadzu DTG-60/60H. The heating rate was maintained at 20˚C/min with using alumina powder as reference material.

IR spectra of magneso-silicate and metal *in situ* doping composites were carried out by mixing the solid with potassium bromide in ratio 1:5 and ground to a very fine powder. A transparent disc was formed in a moisture-free atmosphere. The FTIR spectra were recorded using BOMEMFTIR spectrometer in the range 400–4,000 cm^{-1}.

X-ray diffraction patterns of magneso-silicate and metal *in situ* doping composites were carried out using a Shimadzu XD-D1, X-ray diffractometer with Cu-K_α radiation tube source ($\lambda = 1.5406$ Å) and graphite monochromator operating at 30 kV and 30 mA. The measurements were done in 2θ ranges from 5 to 90 with scan speed 2˚/min.

2.4. Sorption and equilibrium time

All the measurements of equilibrium were done by shaking 0.05 g of MgSi ion exchanger with 2.5 ml of Ni^{2+}, Co^{2+}, and Cd^{2+} ion solutions in a shaker thermostat at 25 ± 1˚C with $V/m = 50$ ml/g and natural pH due to these optimum conditions. After each time interval, the shaker is stopped and the solution is separated at once from the solid. The filtrate was taken to analyze for the determination of the concentration of the metal ions by atomic absorption spectrometer (AAS).

2.5. Effect of batch factor and/or composite dose (V/m)

Batch factor was optimized by shaking different weights of composite with different volume of Ni^{2+}, Co^{2+}, and Cd^{2+} ion solutions (50 ppm) to obtain varying V/m ratios (V/m = 25, 50, 100, 200, and 400 ml/g). After an equilibrium, the solutions were separated and the filtrate was taken to analyze for the determination of the concentration of the metal ions by AAS.

2.6. Capacity measurements

Repeated batch equilibration of 50 ppm metal chloride solutions Ni^{2+}, Co^{2+}, and Cd^{2+} ions with the solid material in V/m ratio 50 ml/g was carried out for the capacity evaluation. The mixture was shaken in a shaker thermostat at 25 ± 1°C and natural pH due to these optimum conditions. After overnight standing, the solid was separated and the concentration of the metal ions was measured by AAS. The capacity value was calculated by the following equation:

$$\text{Capacity} = \text{Uptake} \times C_o \times \frac{V}{m}\ \text{mg/g} \tag{1}$$

where C_o is the initial concentration of the ions in solution, V is the solution volume, and m is the mass ion exchangers.

2.7. Distribution and selectivity studies

The distribution coefficient (K_d) of some heavy metals such as Ni^{2+}, Co^{2+}, and Cd^{2+} ions on magneso-silicate sorbent was determined by batch equilibration. The mixture was placed in shaker thermostat adjusted at 25 ± 1°C for 30 min (time within an equilibrium was attained). After equilibrium, the solutions were separated by centrifugation. Ni^{2+}, Co^{2+}, and Cd^{2+} ion concentrations were determined by AAS. The distribution coefficient (K_d) and Separation factor (α_B^A) were calculated using the following equations:

$$K_d = \frac{(A_o - A_{eq.})}{(A_{eq.})} \times \frac{V}{m}\ \text{ml/g} \tag{2}$$

$$\text{Separation factor}\,(\alpha_B^A) = K_d\,(B)/K_d\,(A) \tag{3}$$

where A_o and $A_{eq.}$ are the concentrations of the ions in solutions before and after equilibration, respectively, V is the solution volume, m is the exchanger mass, and K_d (A) and K_d (B) are the distribution coefficients for the two competing species A and B in the ion-exchange system.

2.8. Sorption isotherm studies

Sorption isotherms of Ni^{2+}, Co^{2+}, and Cd^{2+} ions on magneso-silicate sorbent were determined over the entire concentration range (5×10^{-4} to 10^{-1} M) at constant V/m ratio of 50 ml/g. The experiments were carried out in shaker thermostat at 25 ± 1°C. The equilibrium concentration ($C_{eq.}$) and amount uptake (W/m) were calculated in mmol/g as follows:

$$\frac{W}{m} = \text{uptake} \times C_o \times \frac{V}{m}\ \text{mmol/g} \tag{4}$$

$$C_{eq.} = C_o \times [(1 - \text{uptake})]/100 \tag{5}$$

where C_o is the initial concentration of ions (M), V is the solution volume (ml), and m is the mass of the exchanger (g). Plot of C against C/W and/or log $C_{eq.}$ against log W/m were performed to obtain the required isotherm.

3. Results and discussion

The scope of this work was the attempt to synthesize a high chemical stable inorganic ion-exchange material with high selectivity for some heavy metals. Inorganic ion-exchange materials magneso-silicate (MgSi) and metal *in situ* doping composites Ni-MgSi, Co-MgSi, and Cd-MgSi have been synthesized with complete characterization for the four ion-exchange materials.

IR spectra of MgSi, Ni-MgSi, Co-MgSi, and Cd-MgSi composites were represented in Fig. 1. In this figure, five characteristic bands can be observed in the regions ~2,800 − 3,625, ~1,625, ~1,000, 780, and ~480 cm^{-1}. The main absorption band observed for MgSi, Ni-MgSi, Co-MgSi, and Cd-MgSi at 3,625–2,820 cm^{-1} can be attributed to the stretching mode of free water and OH groups absorbed on the composites. The intensity of this band is decreased by the *in situ* doping of Ni^{2+}, Co^{2+}, and Cd^{2+} ions with magneso-silicate composite. The strong bands appear at ~1,625 cm^{-1} represents the bending mode of water molecules absorbed on MgSi, Ni-MgSi, Co-MgSi, and Cd-MgSi [10]. The absorption band at 1,000 cm^{-1} is due to the metal-oxygen bonds [11–18]. The band at ≈780 cm^{-1} is due to the Mg–OH deformation vibration or overlapping of the Si–O and Si–OH [15–19], and Mg–O bonds in the structure [20]. The bands at 567

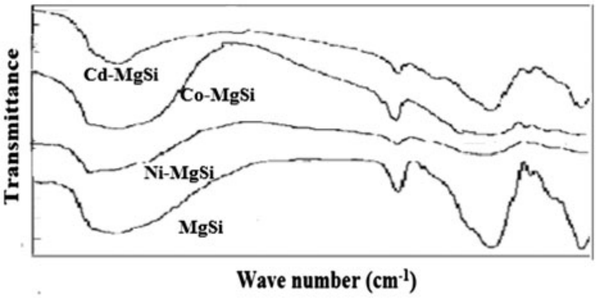

Fig. 1. IR spectra of magneso-silicate and *in situ* doping composite.

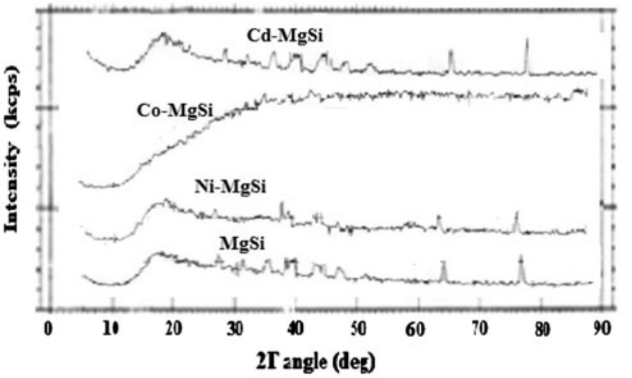

Fig. 2. XRD patterns of magneso-silicate and *in situ* doping composites.

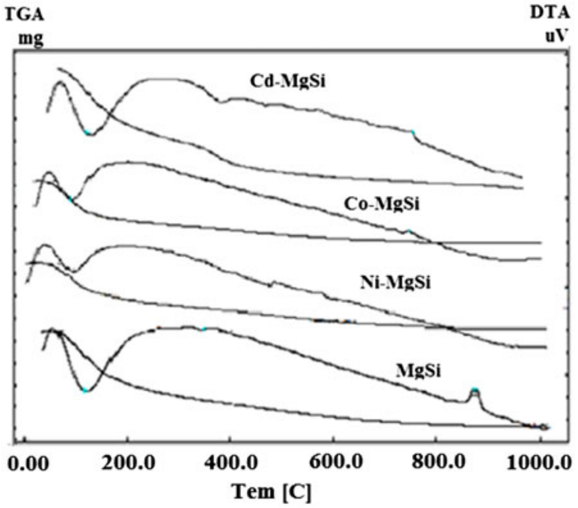

Fig. 3. DTA and TGA for magneso-silicate and *in situ* doping composites.

and 480 cm^{-1} are assigned to Si–O–Mg and Si–O–Si bending vibrations, respectively [19]. The bands between 416 and 465 cm^{-1} are associated with metal-oxygen bonds (Ni–O, Co–O, Cd–O) [21,22].

X-ray diffraction of MgSi, Ni-MgSi, Co-MgSi, and Cd-MgSi composites was represented in Fig. 2. From this figure, it is clear that magneso-silicate and metal *in situ* doping composites M-MgSi have crystalline structure. The crystallinity of magneso-silicate was increased by *in situ* doping of Ni^{2+} and Cd^{2+} ions and decreased with the *in situ* doping of Co^{2+} with magneso-silicate. This variation may be related to the role of ion radius of *in situ*, where the radius of Co^{2+} ion is smaller than Ni^{2+} and Cd^{2+} ions. This means that the ions hold with the water in the texture of the composite according to unhydrated order $Co^{2+} > Ni^{2+} > Cd^{2+}$ and leads to an increase in the water content and weakness of the crystallinity. These results were agreed with the data obtained from XRD of composites materials treated at different heating temperature [6]. The crystallinity of the prepared materials slightly improved with the increase in heating temperatures from 50℃ to 850 ± 1℃, and there is a sharp improvement of crystallinity occurs at 850 ± 1℃.

Differential thermal and thermogravemetric analyses (DTA and TGA) of magneso-silicate and metal *in situ* doping composites were given in Fig. 3. In DTA curve of MgSi (Fig. 3), one endothermic peak is appeared at 104.92℃. This peak may be due to the loss in water molecule [23]. Exothermic peak at 333.92℃ may be due to the decomposition of residual OH-groups and condensation of non-bonded oxygen [24]. Another exothermic peak appeared at 862.09℃ mainly attributed to the formation of crystalline mixed oxide [6]. The DTA curve of Ni-MgSi (Fig. 3), two endothermic peaks are appeared at 100.82 and 472.58℃. The first peak may be due to the loss in water molecule [23] and the second peak is due to the loss of chemical bond water [25]. Two exothermic peaks appeared at 210.3 and 512.2℃. The first peak may be due to the decomposition of residual OH-groups and condensation of non-bonded oxygen [24] and the second peak may be due to the phase change to metal oxide. The DTA curve of Co-MgSi (Fig. 3), one endothermic peak is appeared at 86.77℃. This peak may be due to the loss in water molecule [25]. Two exothermic peaks are appeared at 210.3 and 745.46℃. The first peak may be due to the decomposition of residual OH-groups and condensation of non-bonded oxygen [24] and the second peak may be due to the phase change to metal oxide. The DTA curve of Cd-MgSi (Fig. 3), two endothermic peaks are appeared at 107.31 and 376.45℃. The first peak may be due to the loss in water molecule and the second peak is due to the loss in chemical bond water [25]. One exothermic peak appeared at 770.01℃ that may be due to the phase change to metal oxide.

From the data of TGA in Fig. 3, it was found that the weight losses for magneso-silicate and *in situ* doping composites are continued up to 700℃, and no weight loss occurred in the range ~700–1,000℃. This supporting the fact that MgSi, Ni-MgSi, Co-MgSi, and Cd-MgSi have a good thermal stability comparing with the other inorganic ion exchangers. The weight loss of MgSi, Ni-MgSi, Co-MgSi, and Cd-MgSi with the heating temperature indicates that a 17.325, 17.22, 19.53, and 15.92% weight loss is obtained when the sample is calcinated at 800℃ for MgSi, Ni-MgSi, Co-MgSi, and Cd-MgSi, respectively.

Table 1
The proposed molecular formulas for magneso-silicate and *in situ* doping composites

Composite	Molecular formula
Magneso-silicate	$MgSi_{4.26}O_{9.53}\cdot 2.17\ H_2O$
Nickel magneso-silicate	$Ni_{2.36}Mg_{0.043}Si_{2.91}O\cdot 1.29\ H_2O$
Cobalt magneso-silicate	$Co_{1.45}Mg_{0.03}Si_{2.7}O\cdot 1.26\ H_2O$
Cadmium magneso silicate	$CdMg_{0.059}Si_{1.24}O_{1.12}\cdot 0.83\ H_2O$

The chemical composition of MgSi, Ni-MgSi, Co-MgSi, and Cd-MgSi based on the elemental analysis obtained from X-ray fluorescence spectrometer and DTA–TGA thermograms whose mass loss permitted calculating the amount of water contained in the matrix by the expression:

$$18n = \frac{X(M + 18n)}{100} \tag{6}$$

where X is the percent mass loss of the water, n is the number of moles of water, and M is the molar mass of the compound without water molecules [26]. An X value was found 11.6, 8.93, 11.32, and 8.23% for MgSi, Ni-MgSi, Co-MgSi, and Cd-MgSi, respectively. The molecular formulas of magneso-silicate and metal *in situ* doping composites were calculated and tabulated in Table 1.

The variation of adsorption percentage of Ni^{2+}, Co^{2+}, and Cd^{2+} ions onto magneso-silicate with shaking time was carried as shown in Fig. 4. It is seen that the percent uptake increases with the increase in shaking time and maximum adsorption was observed at 25 min for Cd^{2+} ion and at 30 min for Ni^{2+} and Co^{2+} ions on magneso-silicate. Therefore, we can consider that these times are sufficient to attain equilibrium for Ni^{2+}, Co^{2+}, and Cd^{2+} ions onto magneso-silicate and used for all further experiments.

Effect of batch factor and/or composite dose (V/m) on the percent uptake of Ni^{2+}, Co^{2+}, and Cd^{2+} ions onto magneso-silicate ion exchanger was investigated using V/m ratio's 25, 50, 100, 200, and 400 ml/g. The results were represented in Fig. 5. From this figure, it is clear that retention of Ni^{2+}, Co^{2+}, and Cd^{2+} ions on the magneso-silicate ion exchanger decreases with increasing the V/m ratio and the ratio 25 ml/g is the best ratio for maximum retention value.

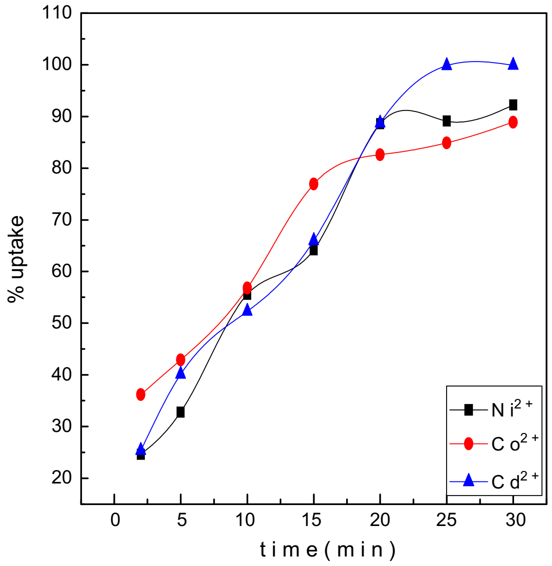

Fig. 4. Effect of contact time on % uptake of Ni^{2+}, Co^{2+}, and Cd^{2+} ions onto magneso-silicate at 25 ± 1°C.

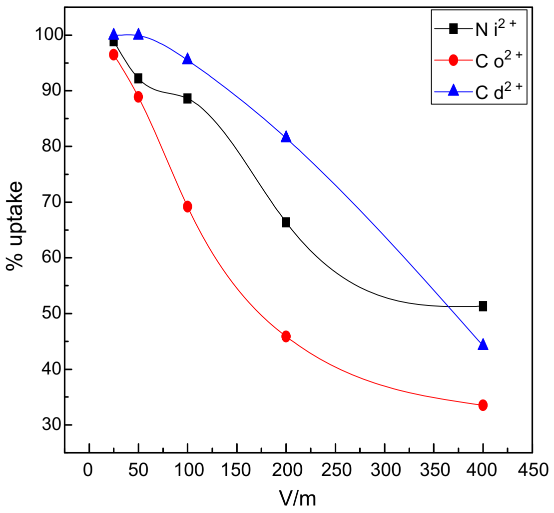

Fig. 5. Effect of V/m on % uptake of Ni^{2+}, Co^{2+}, and Cd^{2+} ions on the MgSi ion exchanger at 25 ± 1°C.

The capacity of magneso-silicate for Ni^{2+}, Co^{2+}, and Cd^{2+} ions was determined at 25 ± 1°C and natural pH due to these optimum conditions. The data are represented in Table 2. Table 2 indicated that the affinity sequence for all cations is $Co^{2+} > Ni^{2+} > Cd^{2+}$. This sequence is in accordance with the unhydrated radii of the exchanging ions. The ions with smaller unhydrated radii easily enter the pores of the exchanger, resulting in higher adsorption [27]. The high capacity of magneso-silicate for cobalt ion may be due to the higher complexing ability of cobalt with the presence in more than one oxidation state.

The capacity of *in situ* doping composites metal magneso-silicate for Ni^{2+}, Co^{2+}, and Cd^{2+} ions was studied and the results are tabulated in Table 2. The data in Table 2 showed that the capacity of Ni-MgSi and Co-MgSi composites for Ni^{2+}, Co^{2+}, and Cd^{2+} ions

Table 2
Capacities of magneso-silicate and *in situ* doping composites for Ni^{2+}, Co^{2+}, and Cd^{2+} ions at 25 ± 1℃

Ion exchangers	Water content (%)	Cation	Capacity (mg/g)
MgSi	17.33	Ni^{2+}	9.0125
$MgSi_{4.26}O_{9.53}\cdot 2.17\ H_2O$		Co^{2+}	10
		Cd^{2+}	8.4375
NiMgSi	17.22	Ni^{2+}	0.3
$Ni_{2.36}Mg_{0.043}Si_{2.91}O\cdot 1.29\ H_2O$		Co^{2+}	3.51
		Cd^{2+}	2.37
CoMgSi	19.53	Ni^{2+}	5.65
$Co_{1.45}Mg_{0.03}Si_{2.7}O\cdot 1.26\ H_2O$		Co^{2+}	6.1175
		Cd^{2+}	4.81

is lower than that obtained for MgSi by 0.21 and 0.6 values, respectively, with the sequence order; $Co^{2+} > Ni^{2+} > Cd^{2+}$ for Co-MgSi and the sequence order; $Co^{2+} > Cd^{2+} > Ni^{2+}$ for Ni-MgSi. These results suggest that the composite keeps cavity for exchangeable ions in the framework by *in situ* doping of these cations with MgSi. The product will show selectivity for the exchangeable ions just as to be retained in ion memory after exchanging particular ion with other ion to maintain fundamentally original structures by *in situ* doping of these cations with MgSi. Similar results were obtained by Abou-Mesalam and El-Naggar for magneso-and magnesium alumino-silicates [6].

Distribution coefficient is an important parameter to explore the separation potentiality of magneso-silicate for Ni^{2+}, Co^{2+}, and Cd^{2+} ions. The distribution coefficients (K_d) and separation factors (α) for the mentioned cations of the range (10^{-3} to 2 M) HNO_3 medium were calculated and tabulated in Table 3. The data in Table 3 indicated that the distribution coefficients have the affinity sequence $Ni^{2+} \geq Co^{2+} \geq Cd^{2+}$ for magneso-silicate. This sequence supports the sorption of metal ions in unhydrated state. The separation factors for the studied cations were calculated and indicated that Co^{2+} ion has a higher separation factor.

The data in Table 3 shows the inverse proportion of the removal percentage with the $[H^+]$ ion concentration. The ion mobility of Ni^{2+}, Co^{2+}, and Cd^{2+} ions are decreased by increasing hydrogen ion concentration. The decrease in the ion mobilities may be explained by an increase in the frictional forces exerted on the ions due to the change of the nature of hydrogen bonds in water [28–30]. As the proton concentration increases, the following water cluster ions are formed H_3O^+, $H_5O_2^+$, $H_7O_3^+$, $H_9O_4^+$ modifying the structure of water and thus the ion–water interaction [30]. Also, the sorbent takes up the H^+ ions from the solution; hence, the surface becomes positively charged, which eventually restricts the uptake of Ni^{2+}, Co^{2+}, and Cd^{2+} ions [30].

Table 3
K_d values and separation factors (α) for Ni^{2+}, Co^{2+}, and/or Cd^{2+} ions onto magneso-silicate at 25 ± 1℃

$[H^+]$	K_d ml/g and (α)	Ni^{2+}	Co^{2+}	Cd^{2+}
0.001	K_d	24,950	24,950	2,319.67
	(α)		(1)	(0.09) (0.09)
0.01	K_d	24,950	24,950	158.42
	(α)		(1)	(7×10^{-3}) (7×10^{-3})
0.1	K_d	24,950	24,950	323.15
	(α)		(1)	(0.013) (0.013)
0.5	K_d	24,950	41.24	5.43
	(α)		(0.002)	(2×10^{-4}) (0.1317)
1	K_d	54.17	314.96	60.35
	(α)		(5.82)	(1.12) (0.19)
2	K_d	0.51	39.45	0.5
	(α)		(78.10)	(1.0) (0.013)

The nature of adsorption processes for Ni^{2+}, Co^{2+}, and Cd^{2+} ions on magneso-silicate was investigated by gradual increase in the sorbate concentration and measuring the amount sorbed at each equilibrium concentration. The Freundlich isotherm most widely used mathematical model, given an empirical expression encompassing the surface heterogeneity and exponential distribution of active sites and their energies was tested in the following equation [31]:

$$\log \frac{W}{m} = K + K' \log C_{eq.} \tag{7}$$

where W/m is the amount uptake, $C_{eq.}$ is the equilibrium concentration, K' and K are the Freundlich constants measure the adsorption intensity and

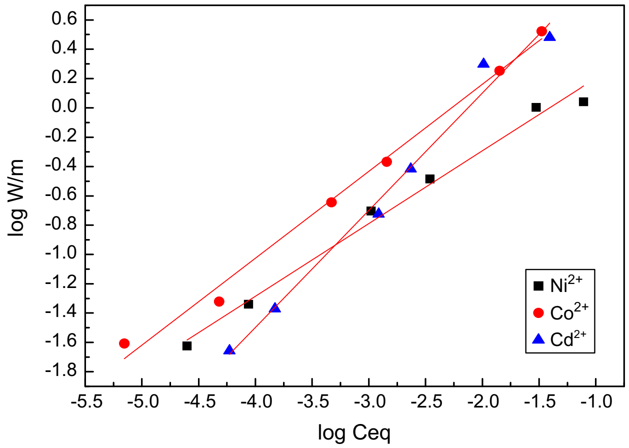

Fig. 6. Freundlich adsorption isotherm for the adsorption of Ni^{2+}, Co^{2+}, and Cd^{2+} ions on magneso-silicate at 25 + 1 ℃.

Table 4
Freundlich parameters for adsorption of Ni^{2+}, Co^{2+}, and Cd^{2+} ions on magneso-silicate at 25 ± 1 ℃

Composite	Ions	K'	K
MgSi	Ni^{2+}	0.49594	0.015
	Co^{2+}	0.59315	0.014
	Cd^{2+}	0.80022	0.015

adsorption capacity of the sorbent, respectively, and computed from the slope and intercept of the linear relationship.

Plots of log W/m against log $C_{eq.}$ linear relationships were obtained for all cases as shown in Fig. 6 for magneso-silicate. The data in Fig. 6 show the applicability of Freundlich isotherm for all cases and all of Ni^{2+}, Co^{2+}, and Cd^{2+} ions are physically sorbed on magneso-silicate. The values of adsorption capacity (K) and adsorption intensity (K') for Ni^{2+}, Co^{2+}, and Cd^{2+} ions on magneso-silicate were computed from the linear relationships in Fig. 6 and tabulated in Table 4. As seen from Table 3, the numerical values of ($K' < 1$) suggest the surface of the sorbent of heterogeneous type [31]. Also the numerical value of (K') is only reduced at lower equilibrium concentrations. Freundlich sorption isotherm does not predict any saturation of the solid surface thus envisages infinite surface coverage mathematically. Similar results were also reported for the adsorption of Zn^{2+}, Cu^{2+}, Cd^{2+}, and Ni^{2+} ions on poly acrylamide acrylic acid impregnated with silico-titanate ion exchanger [32] and UO_2^{2+} and Th^{4+} ions on titanium antimonate [33] (Table 4).

Similar results obtained for the value of K' was found to be less than unity for the adsorption of (Pb^{2+} 0.34), (Cd^{2+} 0.29), and (Zn^{2+} 0.16) on antimonic acid [34]. (Cd^{2+} 0.60), (Zn^{2+} 0.89) on iron(III) titanate [35]. (Cu^{2+} 0.86), (Co^{2+} 0.83), (Zn^{2+} 0.79), (Cd^{2+} 0.79), (Cs^{+} 0.86), and (Fe^{3+} 0.71) on magneso-silicate and (Cu^{2+} 0.68), (Co^{2+} 0.59), (Zn^{2+} 0.77), (Cd^{2+} 0.83), (Cs^{+} 0.86), and (Fe^{3+} 0.77) on magnesium alumino-silicate [9].

References

[1] M.M. Abou-Mesalam, Applications of inorganic ion exchangers: II—Adsorption of some heavy metal ions from their aqueous waste solution using synthetic iron (III) titanate, Adsorption 10 (2004) 87–92.
[2] M. Luqman, Ion Exchange Technology I Theory and Materials, King Saud University, Kingdom of Saudi Arabia, 2012.
[3] M.M. Abou-Mesalam, M.A. Hilal, H.A. Arida, Environmental studies on the use of synthesized and natural ion exchange materials in the treatment of drinking and underground water, Arab J. Nucl. Sci. Appl. 46(3) (2013) 63–74.
[4] I.M. Ali, E.S. Zakaria, M.M. Ibrahim, I.M. El-Naggar, Synthesis, structure, dehydration transformations and ion exchange characteristics of iron-silicate with various Si and Fe contents as mixed oxides, Polyhedron 27 (2008) 429–439.
[5] V.J. Inglezakis, S.G. Poulopoulos, Adsorption, Ion Exchange and Catalysis Design of Operations and Environmental Applications, Elsevier, Amsterdam, 2006.
[6] M.M. Abou-Mesalam, I.M. El-Naggar, Selectivity modification by ion memory of magneso-silicate and magnesium alumino-silicate as inorganic sorbents, J. Hazard. Mater. 154 (2008) 168–174.
[7] L.M. Gando-Ferreira, Ion Exchange Technology II: Application, In amuddin, M. Luqman (Eds), Springer Science and Business Media B.V., Coimbra, Portugal, 2012.
[8] Y.K. Lee, Nanoparticles modified by encapsulation of ligands with a long alkyl chain to affect multispecific and multimodal imaging, J. Nucl. Med. 53(9) (2012) 1462–1470.
[9] I.M. El-Naggar, M.M. Abou-Mesalam, Novel inorganic ion exchange materials based on silicates; synthesis, structure and analytical applications of magneso-silicateand magnesium alumino-silicate sorbents, J. Hazard. Mater. 149 (2007) 686–692.
[10] I.M. El-Naggar, M.M. Abou-Mesalam, Synthesis, characterization and ion exchange properties of lithium zirconium silicate as inorganic ion exchanger, Arab J. Nucl. Sci. Appl. 38(3) (2005) 49–60.
[11] I.M. Ali, Y.H. Kotp, I.M. El-Naggar, Sorption mechanism of some heavy metal ions from aqueous media magnesium silicate, Arab J. Nucl. Sci. Appl. 43 (4) (2010) 101–113.
[12] I.M. Ali, Y.H. Kotp, I.M. El-Naggar, Thermal stability, structural modifications and ion exchange properties of magnesium silicate, Desalination 259 (2010) 228–234.
[13] W. Clowutimon, P. Kitchaya, P. Asswasaengrat, Adsorption of free fatty acid from crude palm oil magnesium silicate derived from rice husk, Eng. J. 15(3) (2011) 15–25.

[14] Y.S. Al-Degs, M.I. El-Barghouthi, A.A. Issa, M.A. Khraisheh, G.M. Walker, Sorption of Zn(II), Pb(II), and Co(II) using natural sorbents: Equilibrium and kinetic studies, Water Res. 40 (2006) 2645–2658.

[15] D.M. Ibrahim, S.A. El-Hemaly, F.M. Abdel-Kerim, Study of rice-husk ash silica by infrared spectroscopy, Thermochim. Acta 37(3) (1980) 307–314.

[16] B.K. Padhi, C. Patnaik, Development of Si_2N_20, Si_3N_4 and SiC ceramic materials using rice husk, Ceram. Int. 21 (1995) 213–220.

[17] B. Stuart, Modern Infrared Spectroscopy, John Willy & Sons, New York, NY, 1996.

[18] J. Madejová, FTIR techniques in clay mineral studies, Vib. Spectrosc. 31 (2003) 1–10.

[19] I.M. El-Naggar, N. Belacy, M.M. Abou-Mesalam, H.F. Aly, Use of selective sorbents for liquid wastes treatment, MRS Proc. 506 (1997) 975–976.

[20] C. Heitner-Wirguin, A. Albu-Yaron, Hydrous oxides and their cation exchange properties—II Structure and equilibrium experiments, J. Inorg. Nucl. Chem. 28 (1966) 2379.

[21] S.A. Nabi, Z.M. Siddiqi, Preparation, properties, and analytical applications of crystalline tin(IV) tungstoselenate, Bull. Chem. Soc. Jpn. 58 (1985) 724–730.

[22] J.P. Rawat, A.A. Ansari, Synthesis and ion exchange properties of sodium stannosilicate: A silver selective inorganic ion exchanger, Bull. Chem. Soc. Jpn. 63 (1990) 1521–1525.

[23] M.M. Ibrahim, MSc Thesis, Faculty of Science, Benha Branch, Zagazig University, Chemistry Department, Banha, Egypt, 2006.

[24] M.M. Abou-Mesalam, Sorption kinetics of copper, zinc, cadmium and nickel ions on synthesized silico antimonate ion exchanger, Colloids Surf. A: Physicochem. Eng. Aspects 225 (2003) 85–94.

[25] M.M. Abou-Mesalam, Structural and crystallographic features of chemically synthesized cero- and titanium cero- antimonates inorganic ion exchangers and its applications, Adv. Chem. Eng. Sci. 1 (2011) 1–8.

[26] K.G. Varshney, A.A. Khan, M.S. Siddiqui, Synthesis, ion exchange behaviour and characterization of chromium(III) arsenosilicate cation exchanger, Colloids Surf. 36 (1989) 405–416.

[27] S.A. Nabi, S. Usmani, N. Rahman, Synthesis, characterization and analytical applications of an ion exchange material: Zirconium (IV) iodophosphate, Ann. Chim. Fr. 21 (1996) 521–530.

[28] S.M. Nomanbhay, K. Palanisamy, Removal of heavy metal from industrial wastewater using chitosan coated oil palm shell charcoal, Electron. J. Biotechnol. 8(1) (2005) 43–53.

[29] O.S. Amuda, A.A. Giwa, I.A. Bello, Removal of heavy metal from industrial wastewater using modified activated coconut shell carbon, Biochem. Eng. J. 36 (2007) 174–181.

[30] H. Moloukhia, Use of animal charcoal prepared from the bivalve chaelatura (chaelatura) companyoi in treatment of waste solution containing cesium and strontium ions, J. Rad. Res. Appl. Sci. 3(2) (2010) 343–356.

[31] M.M. Abou-Mesalam, Sorption kinetics of copper, zinc, cadmium and nickel ions on synthesized silico-antimonate ion exchanger, Colloids Surf. A: Physicochem. Eng. Aspects 225 (2003) 85–94.

[32] M.M. Abou-Mesalam, M.M. Moustafa, M.M. Abdel-Aziz, I.M. El-Naggara, Chemical studies on the retention of some heavy metals from simulated waste water using polymeric species impregnated inorganic ion exchanger, Arab J. Nucl. Sci. Appl. 38(3) (2005) 53–62.

[33] G.M. Ibahim, MSc Thesis, Faculty of Science, Cairo University, Cairo, Egypt, 1997.

[34] I.M. El-Naggar, E.A. Mowafy, W.M. El-Kenany, Kinetics and adsorption isotherm of some heavy metal ions from aqueous waste solutions by crystalline antimonic acid, Arab J. Nucl. Sci. Appl. 43(2) (2010) 98–106.

[35] M.M. Abou-Mesalam, S.A. Shady, Chemical *in-situ* precipitation and immobilization technologies of radioactive liquid waste using titanium (IV) antimonate ion exchanger, Arab J. Nucl. Sci. Appl. 37(1) (2004) 101–112.